



LAWRENCE  
LIVERMORE  
NATIONAL  
LABORATORY

# Generation of Single-Cycle Light Pulses

*B.C. Stuart, I. Jovanovic, J.P. Armstrong, B.  
Pyke, J.K. Crane, and R. Shuttlesworth*

**February 13, 2004**

This document was prepared as an account of work sponsored by an agency of the United States Government. Neither the United States Government nor the University of California nor any of their employees, makes any warranty, express or implied, or assumes any legal liability or responsibility for the accuracy, completeness, or usefulness of any information, apparatus, product, or process disclosed, or represents that its use would not infringe privately owned rights. Reference herein to any specific commercial product, process, or service by trade name, trademark, manufacturer, or otherwise, does not necessarily constitute or imply its endorsement, recommendation, or favoring by the United States Government or the University of California. The views and opinions of authors expressed herein do not necessarily state or reflect those of the United States Government or the University of California, and shall not be used for advertising or product endorsement purposes.

This work was performed under the auspices of the U.S. Department of Energy by University of California, Lawrence Livermore National Laboratory under Contract W-7405-Eng-48.

# Generation of single-cycle light pulses

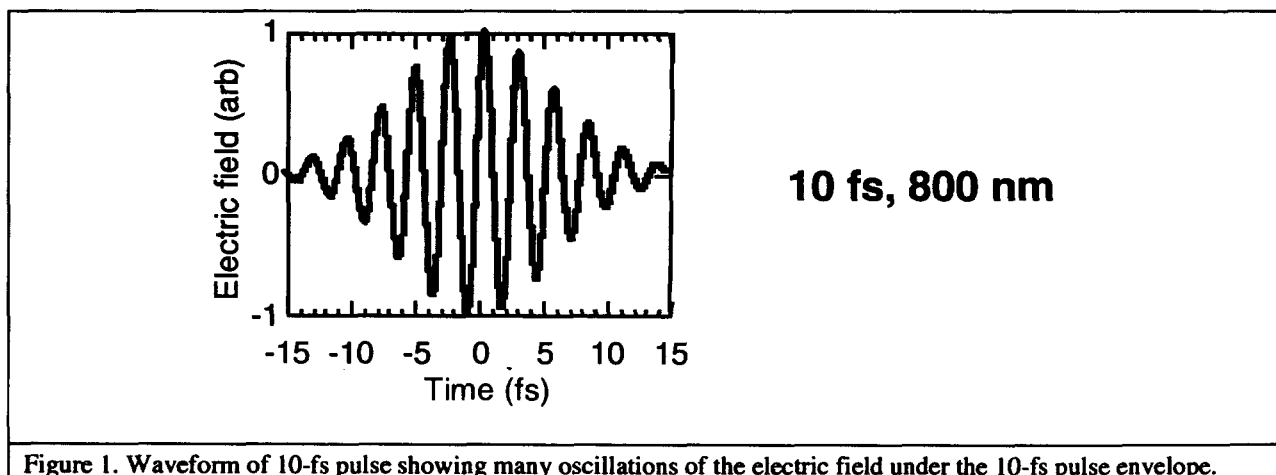
B.C. Stuart, I. Jovanovic, J.P. Armstrong, B. Pyke, J.K. Crane, R. Shuttlesworth  
02-LW-001 Final Report

## I. Abstract

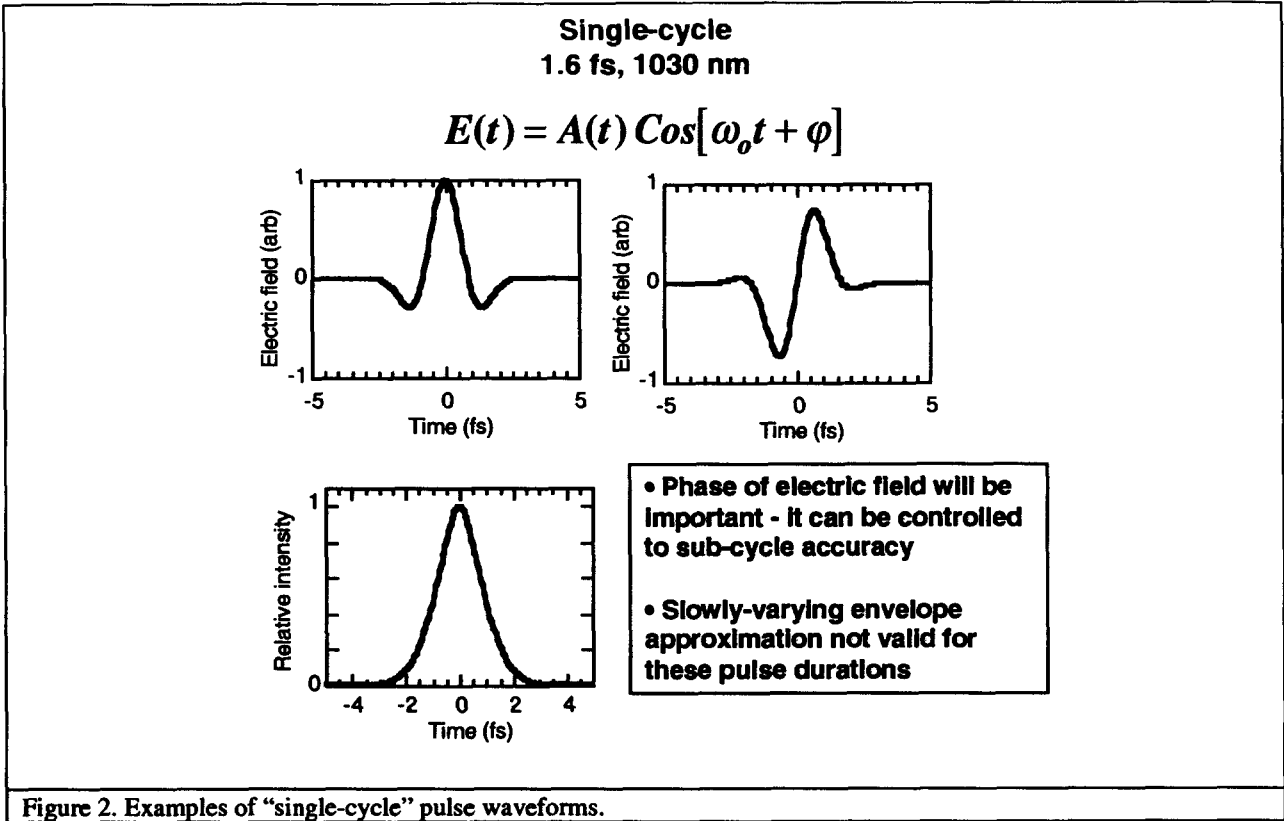
Most optical pulses, even at the 10-femtosecond timescale, consist of several oscillations of the electric field. By producing and amplifying an ultra-broadband continuum, single cycle (< 3 fs) or shorter optical pulses may be generated. This requires a very challenging pulse-compression with sub-femtosecond accuracy. Production of these single-cycle pulses will lead to new generations of experiments in the areas of coherent control of chemical excitations and reactions, 0.1-fs high-order harmonic (XUV) generation for probing of materials and fast processes, and selective 3-D micron-scale material removal and modification. We activated the first stage of a planned three-stage optical parametric amplifier (OPA) that would ultimately produce sub-3 fs pulses. Active control with a learning algorithm was implemented to optimize the continuum generated in an argon-filled capillary and to control and optimize the final compressed pulse temporal shape. A collaboration was initiated to coherently control the population of different states upon dissociation of  $\text{Rb}_2$ . Except for one final optic, a pulse compressor and diagnostics were constructed to produce and characterize pulses in the 5-fs range from the first OPA stage.

## II. Generation of single-cycle pulses

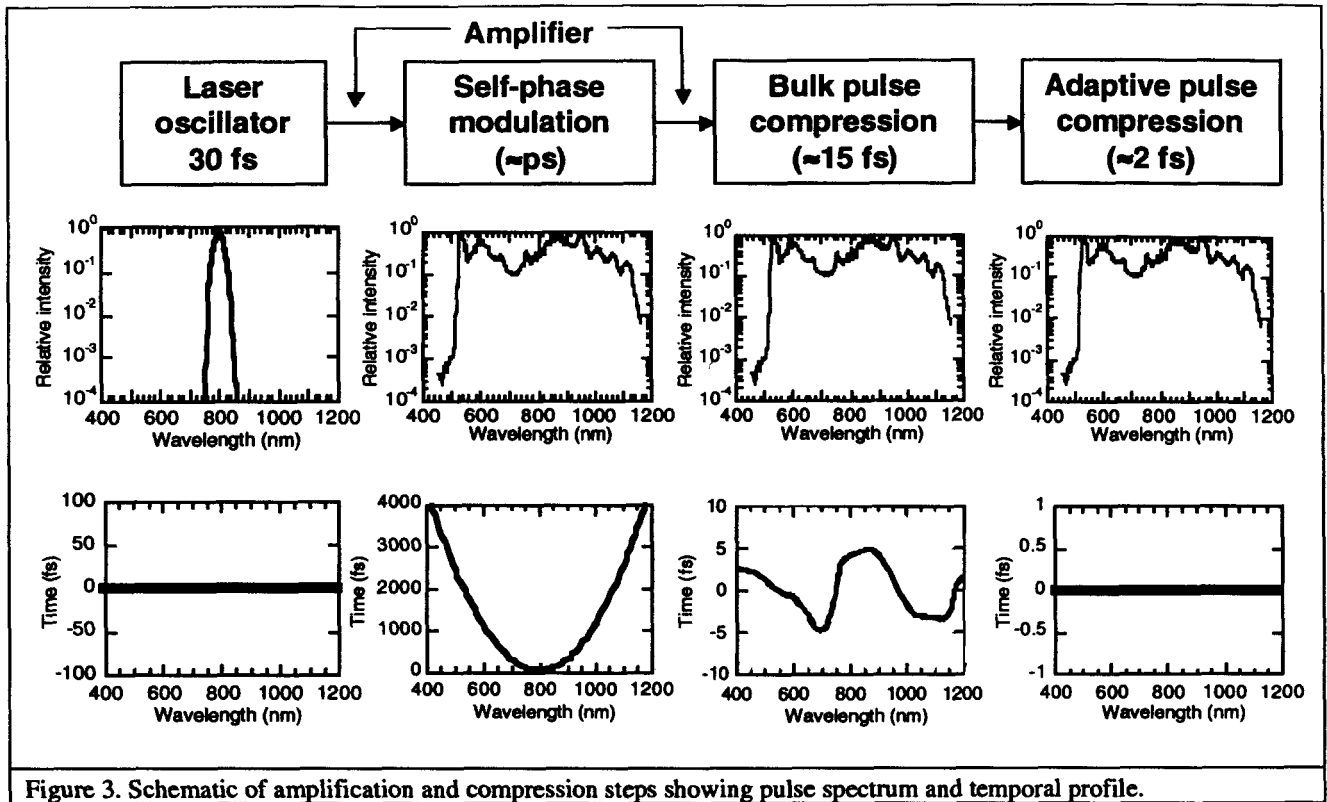
Our main challenge is to generate sufficient bandwidth (> 300 nm) to support the ultrashort pulse duration and then to phase all the frequencies to each other to within a small fraction (<fs) of the desired final pulse duration. The shortest pulses generated directly in a laser oscillator (Ti:sapphire) are approximately 5 fs and centered at 800 nm [1] (800 nm corresponds to  $\nu=3.8 \times 10^{14} \text{ s}^{-1}$ , period=2.7 fs). An example 10-fs pulse wave form is shown in Figure 1.



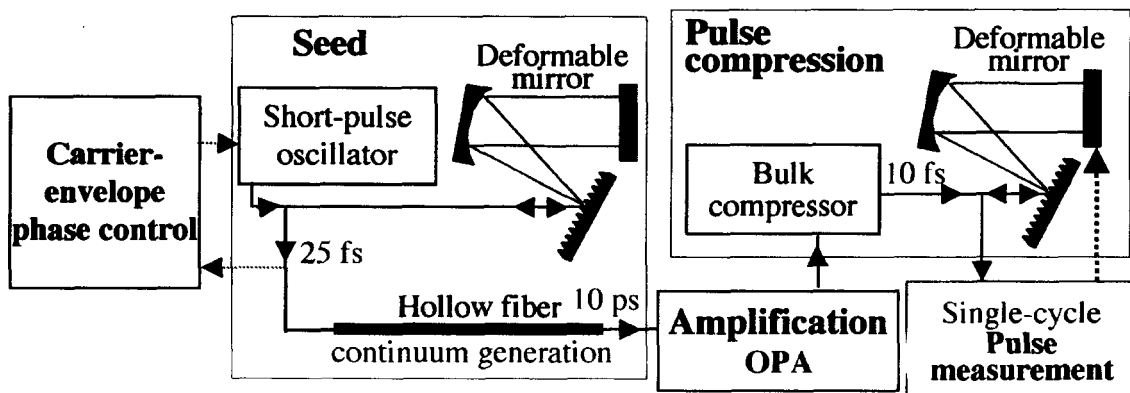
To generate even shorter pulses, more bandwidth is necessary. This has been demonstrated recently by propagating sub-100-fs pulses through a microstructure [2] or argon-filled hollow [3] optical fiber. Calculated examples of “single-cycle” waveforms are shown in Figure 2.



After generation of sufficient bandwidth seed pulses, amplification to the mJ level or higher is desirable necessary for certain applications. This can be accomplished through optical parametric amplification (OPA) [4] and we have identified two promising pathways to extremely broadband amplification. After amplification the pulses must be compressed in time. We designed a bulk compressor in combination with an adaptive-optic controlled compressor for fine adjustment. An schematic of the pulse amplitude and temporal profile through the amplification process is shown in Figure 3.



In addition, we want control of the phase of the electric field in relation to the pulse envelope. This can be accomplished using a servo loop based on a carrier-slip beat signal at 540 nm [5]. A schematic of the pulse generation system is shown in Figure 4. Each portion is discussed below in terms of our accomplishments to date and future plans.



A slightly more detailed schematic of the system we were working toward is shown in Figure 5. It includes a three-stage amplifier based on optical parametric amplification (OPA) that is pumped by two different noncollinear 400-nm beams plus an 800-nm beam. The initial continuum is generated in a hollow capillary and a programmable acoustic-optic dispersion filter (Dazzler) is used for optimization of the spectral content.

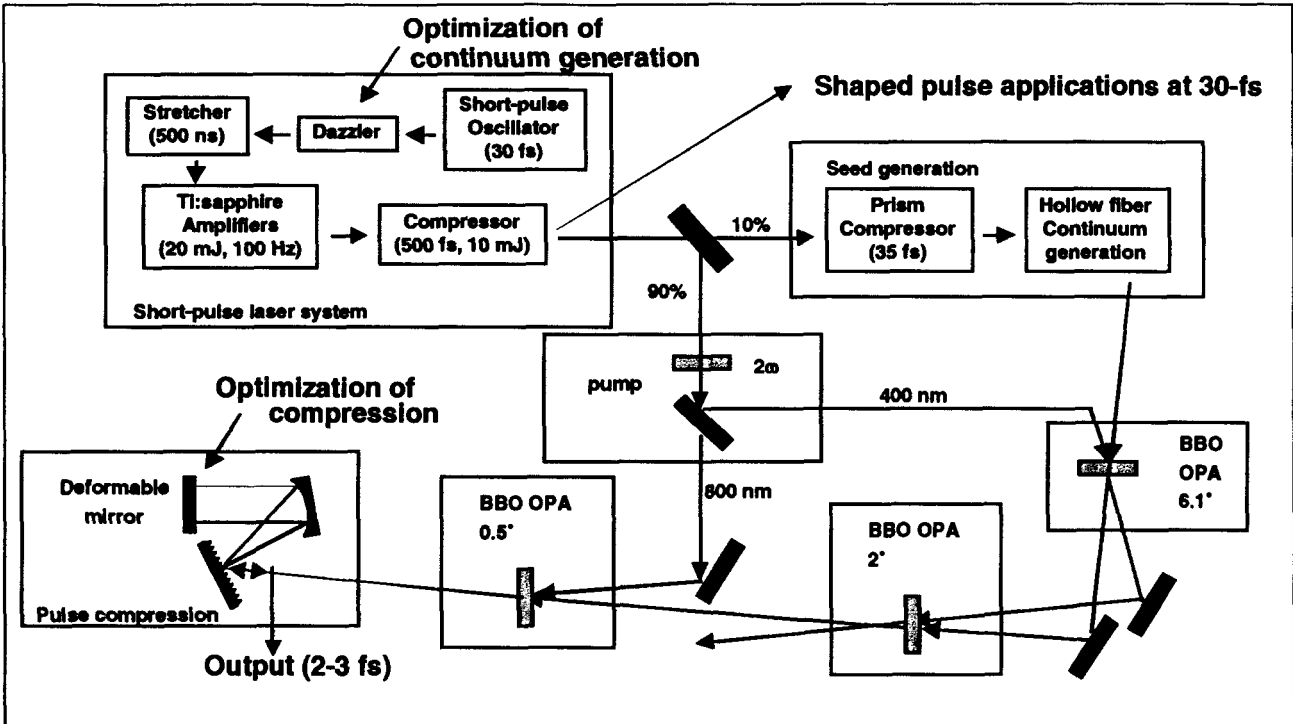


Figure 5. Schematic of system being constructed showing initial continuum generation with 35-fs pulses in hollow fiber and three-stage OPA followed by pulse compressor.

**a. Seed pulses**

There are several methods to generate broad-bandwidth continuum pulses to use as seed pulses into the OPA stages. Focusing into a thin sapphire window is one common method, but the spectral bandwidth achievable is limited by optical damage.

Our original plan was to use a microstructure fiber to generate the necessary bandwidth. By spatially and temporally confining short laser pulses in microstructure fibers, we can generate extremely large continuum bandwidth. The fiber can be tailored for zero or minimal dispersion at the input wavelength, thus confining the pulse longitudinally, Transverse confinement is provided by the fiber guiding. Under these conditions, extremely long interaction lengths allow self-phase modulation, Raman scattering, and four-wave mixing to produce a broad, flat continuum. We set up and demonstrated a very broad continuum spanning 400-1400 nm (Figure 6). The growth of the spectral width as a function of peak power coupled into the microstructure fiber is shown in Figure 7. The single-mode output of the fiber leads to a very high-brightness source.

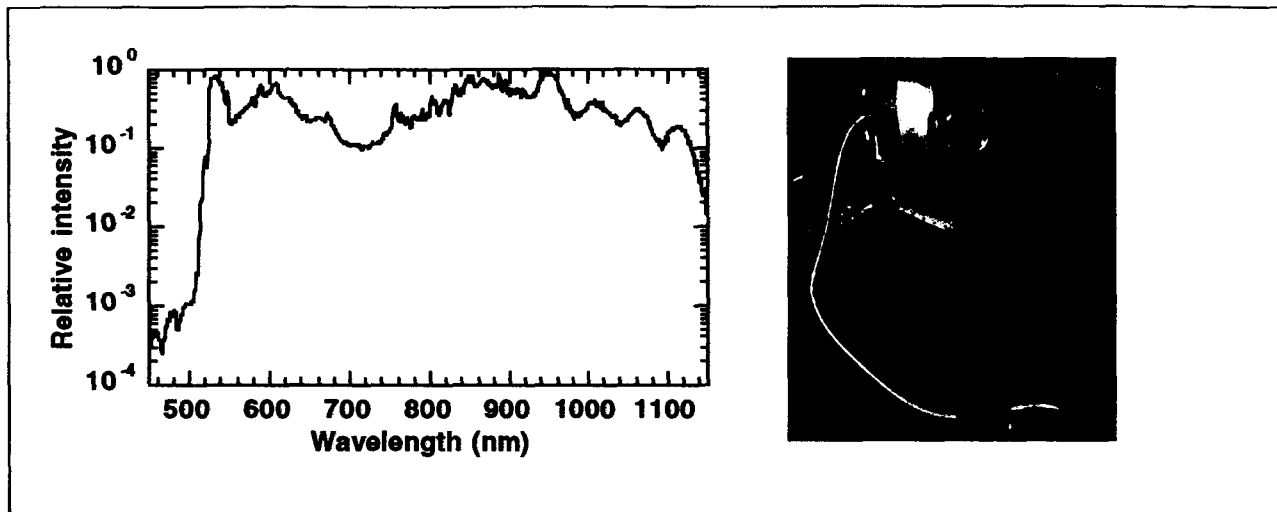


Figure 6, Continuum generation in a microstructure fiber produces extremely broad bandwidth from initial 100-fs (9 nm FWHM) 800-nm pulses.

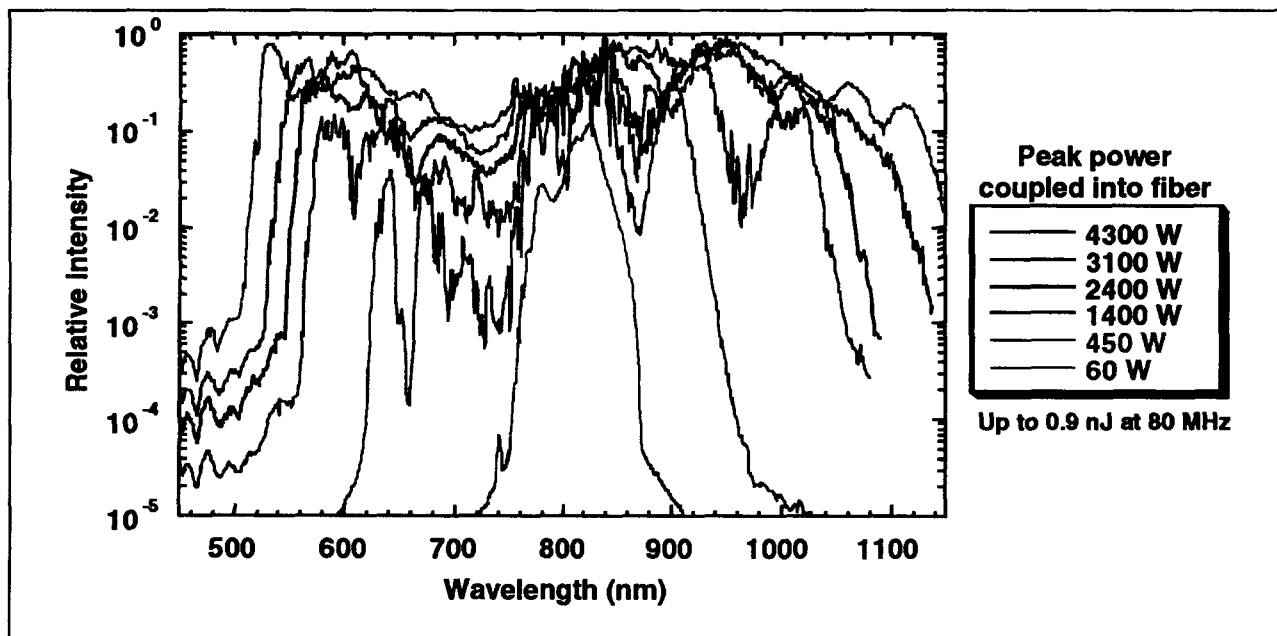
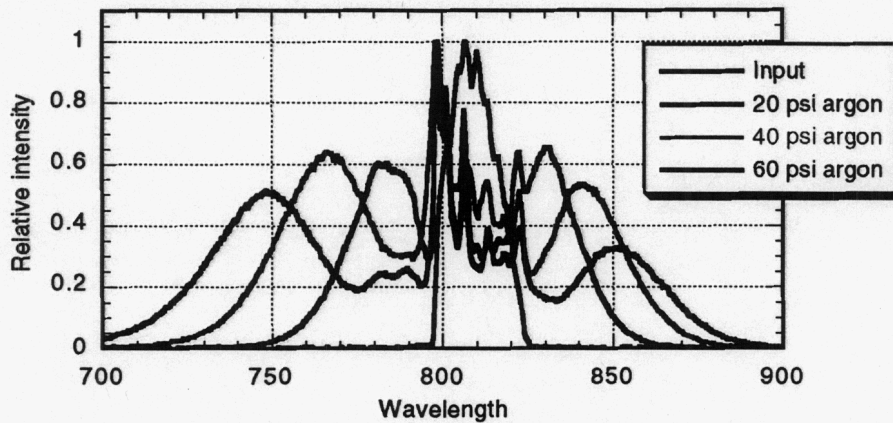
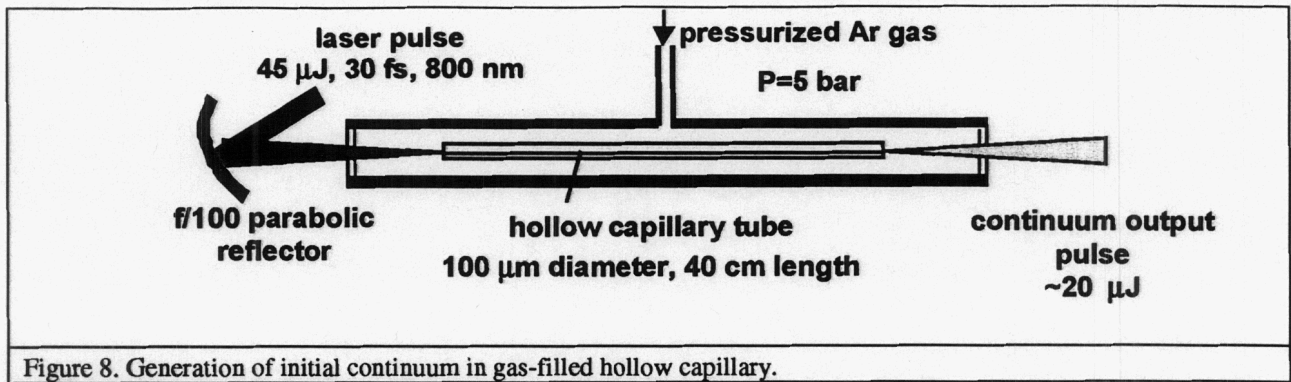


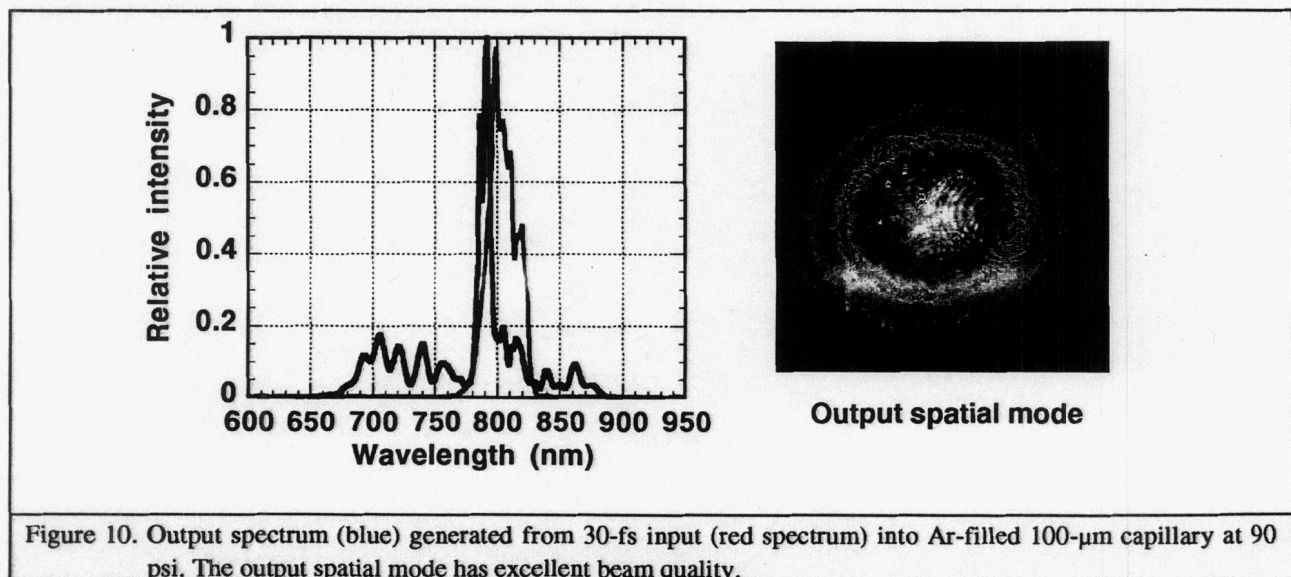
Figure 7. Output spectrum from microstructure fiber as a function of peak power coupled into fiber.

Unfortunately, we learned [6] that the individual pulses that make up this time-averaged (80 MHz) spectrum occur randomly and are extremely spectrally modulated. This modulated spectrum cannot be compressed to our desired transform-limited single-cycle pulse.

The method we settled on to generate the initial spectrum was to inject the amplified pulses from our 30-fs system into an argon-filled hollow capillary (Figure 8). By balancing the gas dispersion and modal dispersion, extremely broad bandwidths can be generated, and the pulses have the correct amplitude and phase [3]. After several attempts with bad fiber, we activated the argon-filled hollow capillary with 150-fs input pulses (Figure 9).



After initial demonstrations of spectral broadening, we upgraded our short-pulse laser system to produce 30-fs pulses and further optimized the continuum generation. Figure 10 shows the spectrum and spatial mode resulting from coupling these 30-fs pulses into a 100- $\mu\text{m}$  core fiber at 90 psi argon.



To further optimize the spectral content of the initial continuum, we implemented closed-loop control, based on a genetic learning algorithm, over the output temporal profile of our short-pulse laser system (input pulses to hollow fiber and pump pulses for OPA). The compressed pulse temporal shape was controlled by the Dazzler. We first used this pulse shaping algorithm to control various spectral attributes of continuum generation in water (Figure 11). This served as a testbed demonstration that our control algorithms functioned properly.

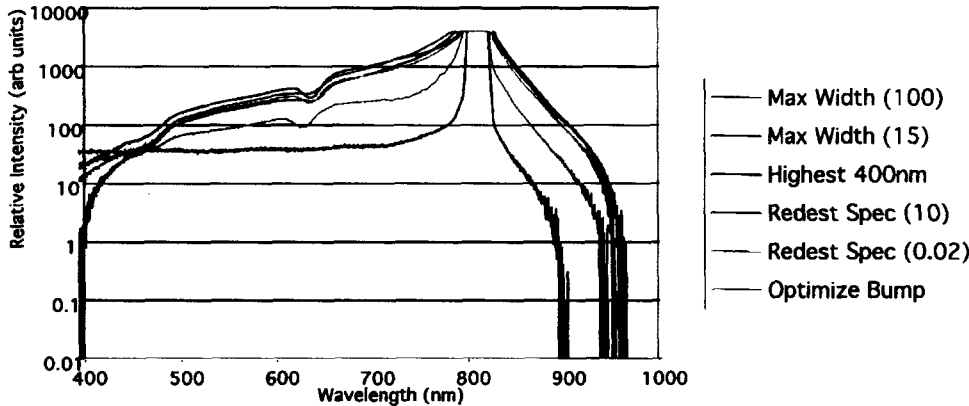


Figure 11. Spectrum produced by focusing 150-fs pulses into water with six different fitness function criteria.

We later used this genetic algorithm to search for the optimum output spectrum from the Ar-filled capillary. The feedback we chose was the Fourier transform of the output spectrum. This method optimizes the compressed-pulse peak power assuming the pulse can be compressed with no phase errors. This was the first time this type of optimization has been performed. Figure 12 shows the initial and optimized spectra generated with nominal 30-fs input pulses.

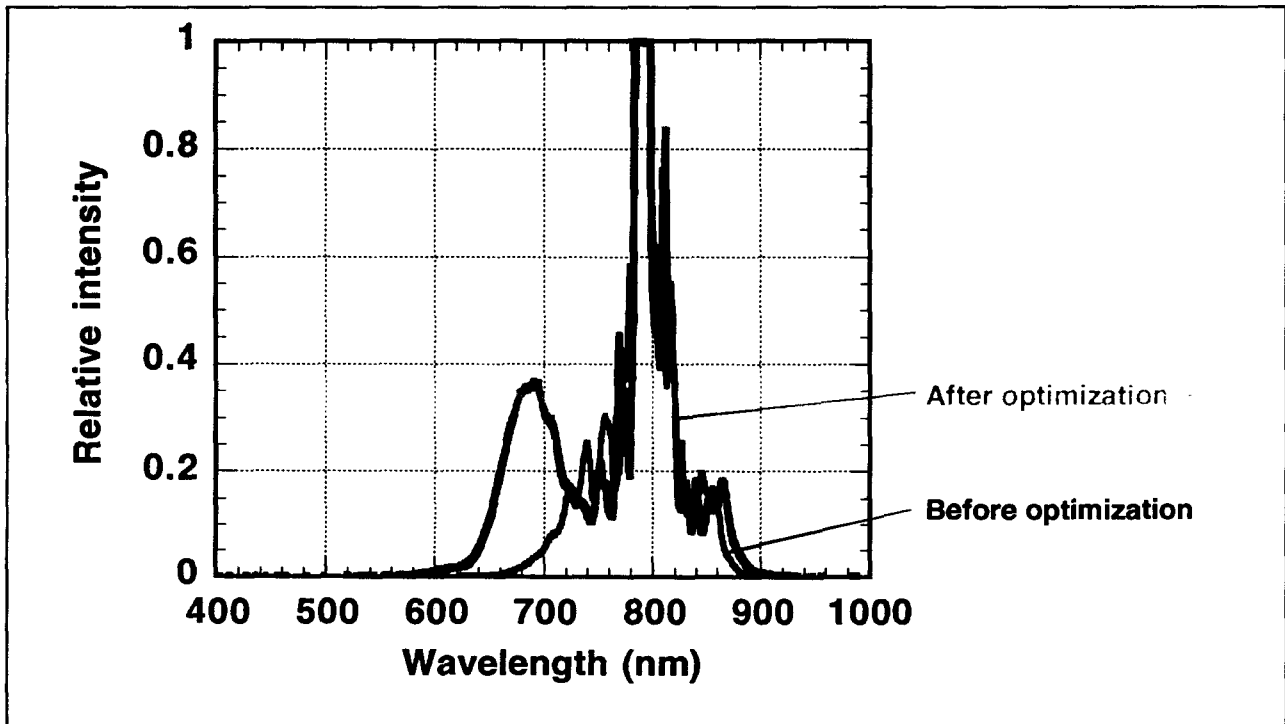


Figure 12. Spectrum from Ar-filled capillary before and after optimization with genetic algorithm that uses Fourier transform of spectrum as feedback.

### b. Amplification

We have numerically investigated advanced techniques for amplification of ultrabroad spectral bandwidth. The motivation for amplifying ultrabroadband pulses stems from possible applications that would benefit from higher energy single-cycle pulses, such as high harmonic generation and coherent control of chemical reactions. We have identified optical parametric amplifiers (OPA) as a technology with the potential to amplify unprecedented bandwidths. In principle, bandwidth of the OPA-based system can be enhanced by using pump sources at different frequencies, noncollinear geometries, and angular dispersion of signal/pump. In Fig. 13 we show the calculated amplified bandwidth in beta-barium borate (BBO) using a 400-nm pump at two different noncollinear angles. Amplification over 300 nm is possible using this scheme. The Fourier transform of this spectrum results in a 5.2-fs compressed pulse.

Even greater amplified bandwidth can be realized by using multiple pumps at multiple wavelengths. The scheme we were working toward is shown in Figure 14. This amplified spectrum will produce 2.5 fs pulses, but with significant temporal wings. We recently fabricated and tested PPKTP (separate LDRD, I. Jovanovic) as a possibility for filling in the central gap in order to generate a more Gaussian temporal profile with greatly reduced wing structure.

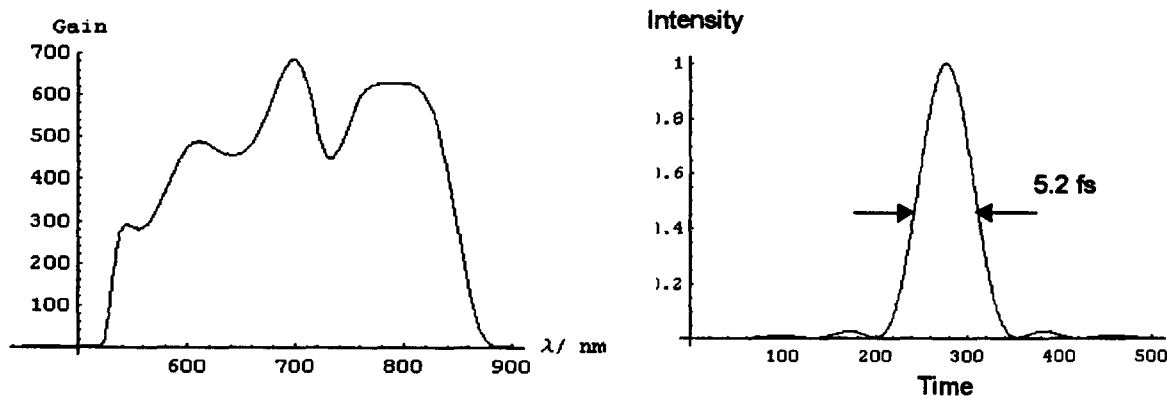


Figure 3. Gain profile in a BBO OPA, pumped with dual 400 nm beams at  $2^\circ$  and  $6.1^\circ$  noncollinear angles. Pump intensity is  $10 \text{ GW/cm}^2$ ; crystal length is 2 mm. The transform-limited compressed pulse duration is 5.2 fs.

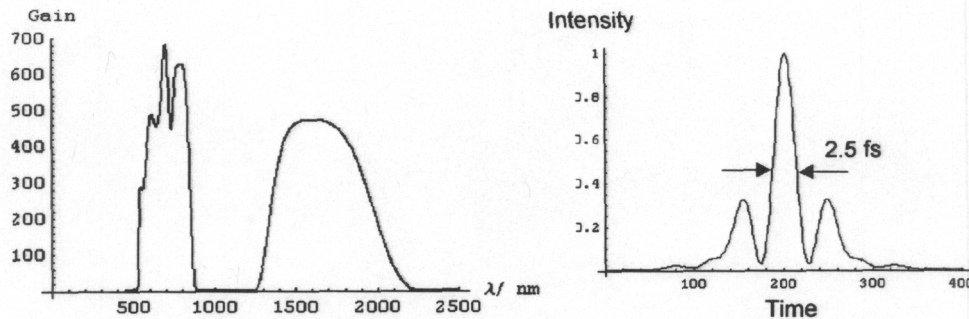


Figure 14. Gain profile in BBO OPA, pumped by a 400-nm beam at 6.1° noncollinear angle, a 400-nm beam at 2° noncollinear angle, and a collinear 800-nm beam. The transform-limited pulse duration is 2.5 fs, but with significant temporal wing structure.

Experimentally, we activated the first stage of OPA amplification using the pulses generated in the argon-filled capillary as the seed and pumping BBO at 400 nm at 6.1° noncollinear angle. Figure 15 shows the experimental arrangement. Stretched pulses from our 100-Hz, 30-fs system at the 15-mJ level were first sent to a grating compressor where they were partially compressed to the 500-fs range. The pulse duration was left at this length to match the expected pulse duration of the continuum seed pulses and to avoid damage and nonlinear effects in the rest of the optical train.

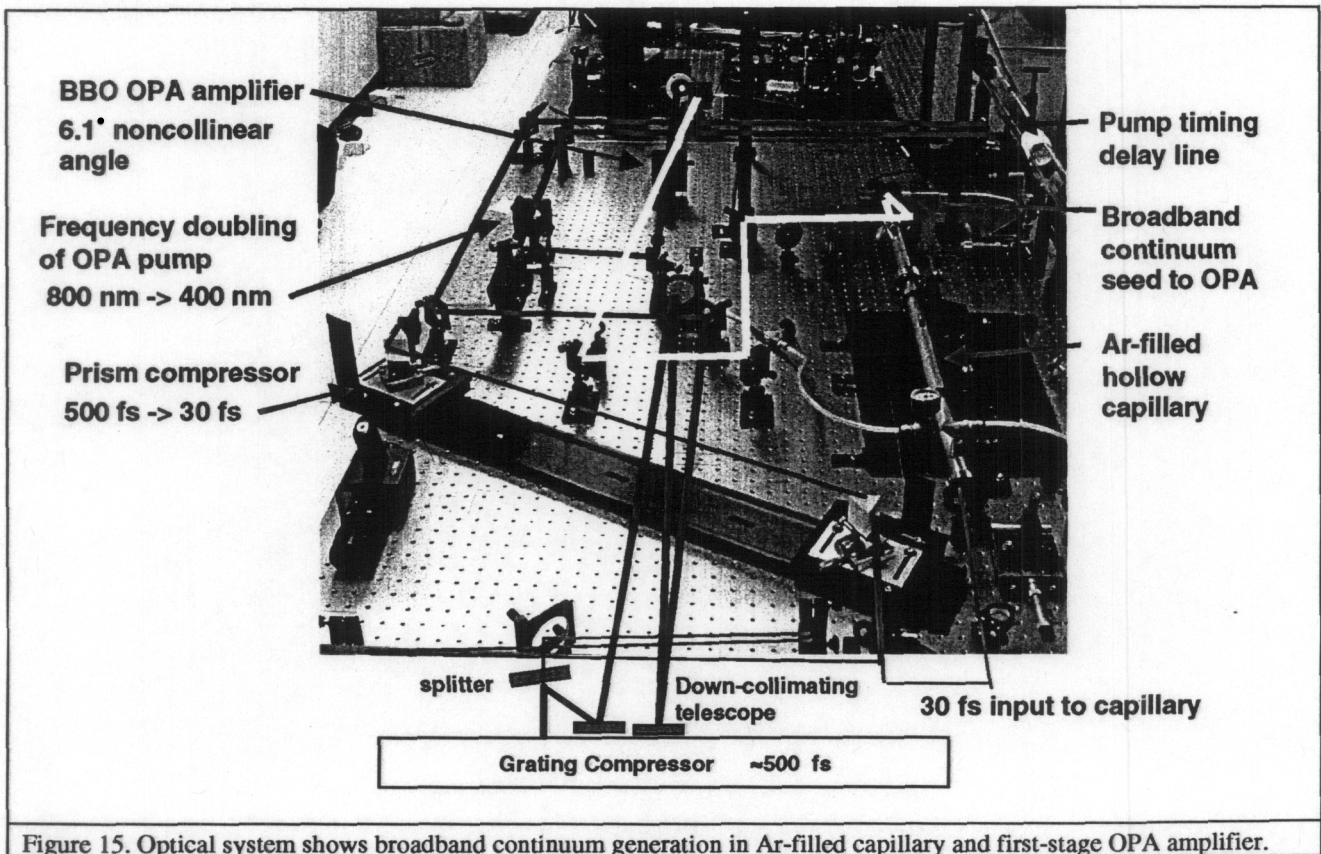
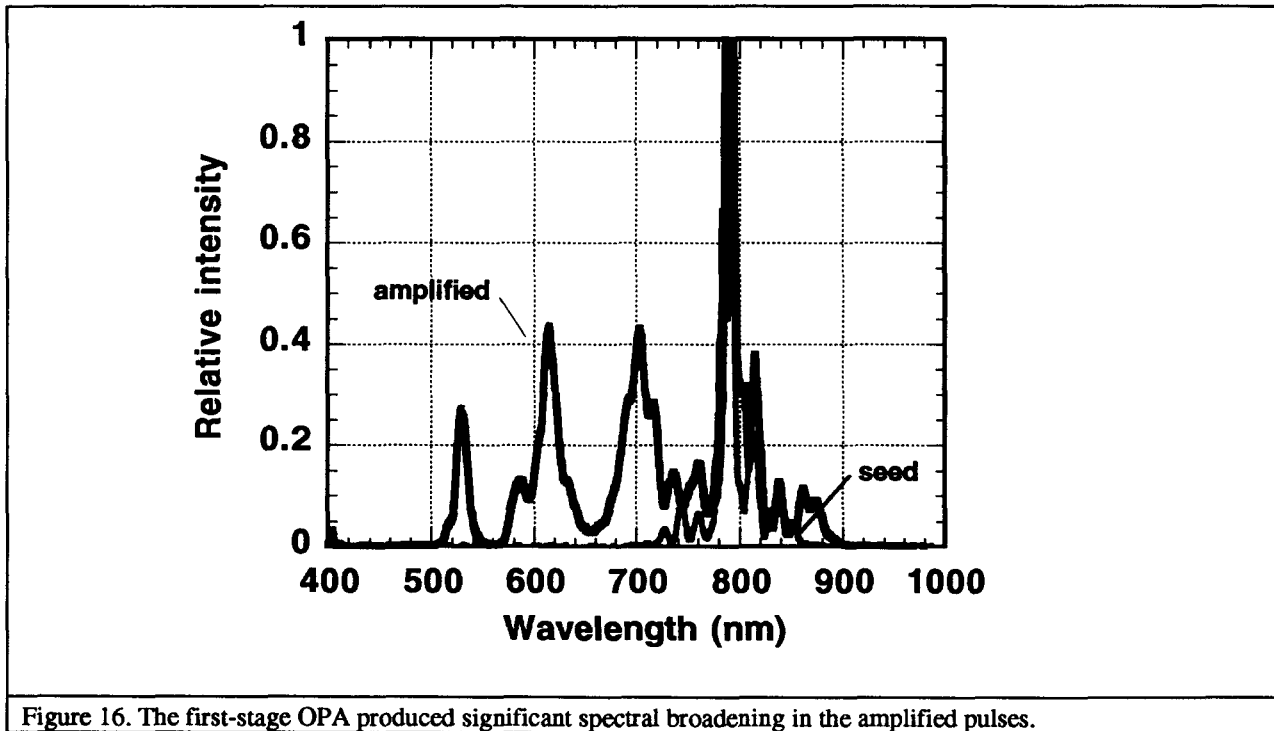


Figure 15. Optical system shows broadband continuum generation in Ar-filled capillary and first-stage OPA amplifier.

The 500-fs pulse was split, with 10% going to the hollow capillary to generate the broadband seed pulses and the other 90% to pump the OPA. The input to the capillary was first compressed

back down to 30-fs using a prism compressor in order to generate the broadest continuum possible. The continuum from the capillary was collimated and directed to seed the OPA. The OPA pump beam was run through a delay line in order to match the path length of the seed to within  $\approx 100$  fs. The 800-nm, 500-fs pulses were frequency-doubled to 400-nm and then down-collimated to pump the OPA with a noncollinear crossing angle of  $6.1^\circ$ .

This first stage of OPA produced a large spectral broadening of the amplified pulses compared to the already-broad seed pulses from the Ar-filled capillary. The amplification shows that although on a linear scale the seed does not appear to have much spectral content below 700 nm, there is a low-level tail that extends throughout the visible range. Amplification of this weak portion of the spectrum combined with the initial broadened region around 800-nm gave us enough bandwidth to compress to approximately 5 fs. Further optimization of the process was planned to try to smooth out the spectrum which would result in compressed pulses with less temporal wing structure.



### c. Pulse compression

A pulse compressor was designed and constructed to compress the  $\approx 500$  fs pulses from the first-stage OPA down to the 5-fs level. This first-generation compressor utilized a diffraction grating, spherical mirror, and deformable mirror in the focal plane (Figure 17). The deformable mirror is used for the fine phase control and final pulse compression optimization. This deformable mirror is used along with the Dazzler in closed-loop control to minimize the final pulse duration

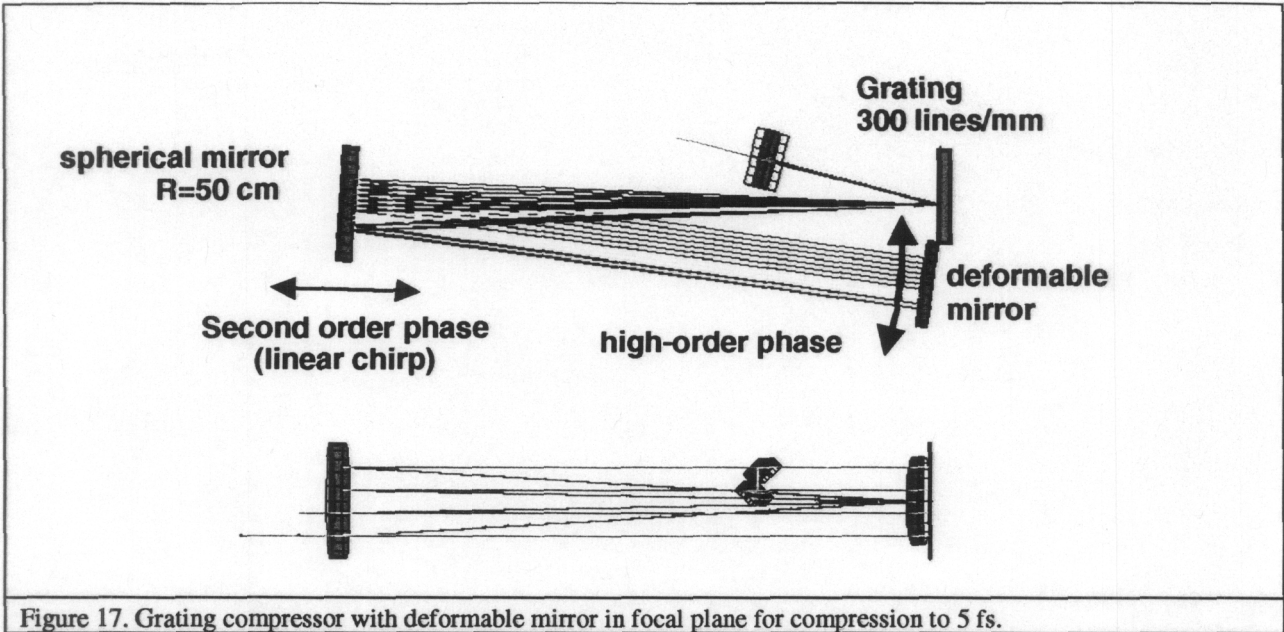


Figure 17. Grating compressor with deformable mirror in focal plane for compression to 5 fs.

To demonstrate operation of the deformable mirror with an optimization algorithm, we first set up to flatten the deformable membrane mirror. We developed a genetic algorithm that runs under the control of LabView instrumentation software. This enables the optimization of multivariable nonlinear processes through active monitoring and control of optical devices. As a demonstration of the genetic algorithm's performance, we employed it to flatten the deformable mirror. The mirror was shipped from the manufacturer with approximately 3 waves of curvature over its surface (Figure 18). The mirror was placed into a Michelson interferometer and a CCD camera was used to count fringes in the interference pattern. The number of fringes appearing in the lineout is a measurement of how closely that configuration matches a flat mirror and is termed an individual's fitness. This individual is made up of genes that encode voltage levels for each of the 19 actuators in the mirror. The algorithm begins by creating an initial random population made up of 48 individuals, which are then tested in sequence to determine the number of fringes produced by each individual's genes. Next, the population is sorted by fitness and only the best six individuals are kept. These six are paired through weighted random pairing and their genes are combined to form new individuals, or offspring. The new population finally goes through a 5% mutation rate in which genes are randomly altered in order to explore new parameter space and avoid local minima. This population is then tested and the process repeats until a convergent solution is found. The genetic algorithm was able to flatten the mirror after 25 generations (Figure 19). This routine forms the basis of our pulse shaping control.

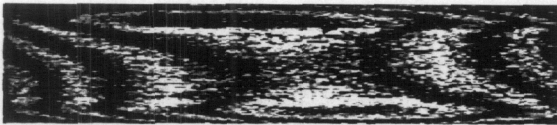


Figure 18: Mirror as shipped with curvature

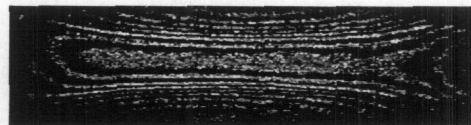


Figure 19: Mirror after running genetic algorithm.

The pulse compressor was assembled (Figure 20) except for a new spherical mirror that was needed to support the broad amplified bandwidth. This mirror was dropped and broken by the vendor and not received before the project was terminated.

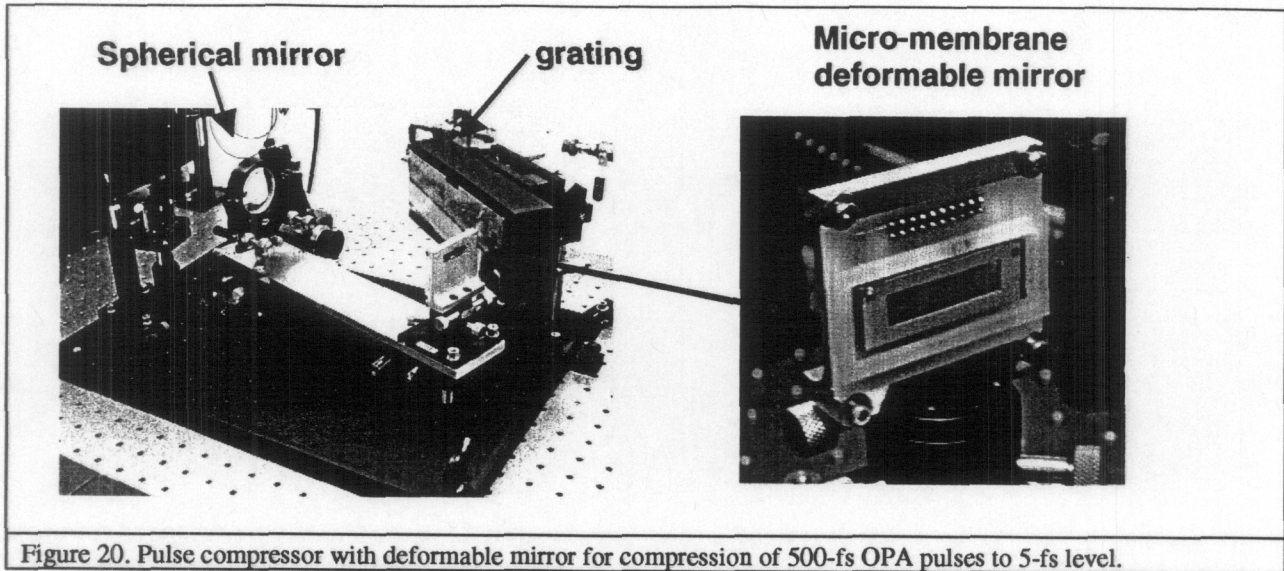
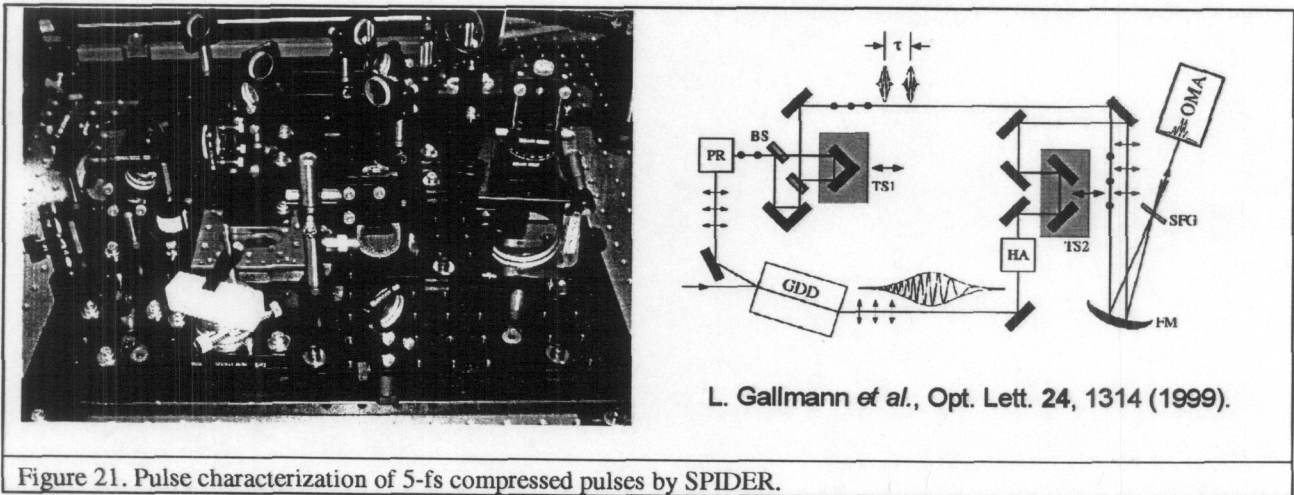


Figure 20. Pulse compressor with deformable mirror for compression of 500-fs OPA pulses to 5-fs level.

#### d. Pulse measurement

Two common techniques, Spectral Phase Interferometry for Direct Electric Field Reconstruction (SPIDER) [7] and Frequency-Resolved Optical Gating (FROG) [8] are used to measure compressed pulses of this type. Both techniques give the pulse amplitude and phase. We have assembled a SPIDER unit for characterization of our 5-fs pulses (Figure 21).



L. Gallmann *et al.*, Opt. Lett. 24, 1314 (1999).

Figure 21. Pulse characterization of 5-fs compressed pulses by SPIDER.

#### e. Carrier-envelope phase control

Many applications, such as high-order harmonic generation, are sensitive to the exact phase of the electric field. This is analogous to the electric field being anywhere between a sine and cosine function. We planned in FY04 to implement control over the phase as published in Ref. 5.

### III. Applications of single-cycle light pulses

Ultrafast laser pulses are the fastest probes available to access fundamental physical, chemical, and biological processes directly in the time domain. Single-cycle pulse will enable a wide range of exciting science and applications as outlined in Figure 22.

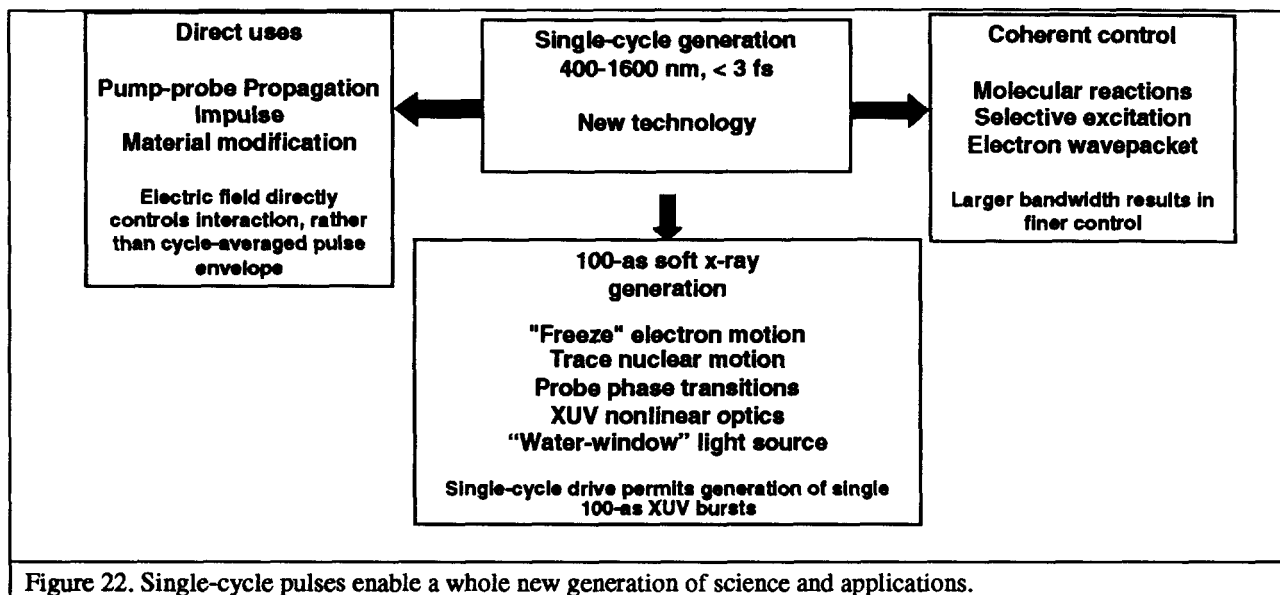


Figure 22. Single-cycle pulses enable a whole new generation of science and applications.

We have identified three uses of immediate interest: selective excitation and detection of chemical compounds, submicron-scale machining of materials, and generation of sub-fs XUV pulses.

Selective excitation of molecules relies on the temporal shaping abilities of this system. With  $\approx 3$  fs transform-limited bandwidth, we will be able to generate longer pulse with  $\approx 3$  fs temporal resolution. Pulses with much lower resolution (15 fs) have been used for selective excitation of closely spaced vibrational modes in  $\text{CO}_2$  [9].

Sub-micron 3-D machining of materials, especially in the bulk of transparent materials, can be achieved by adjusting the spectral phase of the incident pulse so that it is fully compressed (most intense) only at the focal position within the material. This could have application in fusion target sculpting and intercellular cutting (precision scalpel).

High-order harmonics in the XUV can be generated by focusing ultrashort pulses into gases. The harmonics are selectively generated during a small portion of the electric field cycle. Multiple cycles in typical amplified laser pulses result in a pulse train of presumed sub-fs pulses. With a single-cycle drive pulse, single XUV pulses can be generated with durations on the order of 100 as ( $10^{-16}$  s). These pulses would be enabling in probing of fast processes, and should find application in materials probing.

To begin to show the power of coherent control with ultrashort laser pulses, we teamed up with Gary Eden's group at the University of Illinois to study dissociation of  $\text{Rb}_2$  using a new technique based upon four-wave-mixing (FWM). Dissociation is a fundamental process of molecular dynamics and a detailed understanding of the relevant potential surfaces is crucial to ultimately controlling the products. Because FWM is a coherent process it gives the time-

dependent phase and amplitude of the atomic wavepackets produced from dissociation of  $\text{Rb}_2$ , an improvement over earlier techniques based upon laser-induced fluorescence (Zewail). By controlling the phase and amplitude of the laser pump we planned to demonstrate control over the dissociation process by directing the molecule to select a particular pathway (Figure 23). After completing this proof-of-principle experiment (Figure 24) in  $\text{Rb}_2$  we will demonstrate the technique in atmospheric gases such as  $\text{N}_2\text{O}$  or  $\text{NO}_2$ . Using an ultrafast laser with several hundred nm bandwidth, this technique allows simultaneous interrogation of dozens of molecular excited states - *a new paradigm in molecular spectroscopy!*

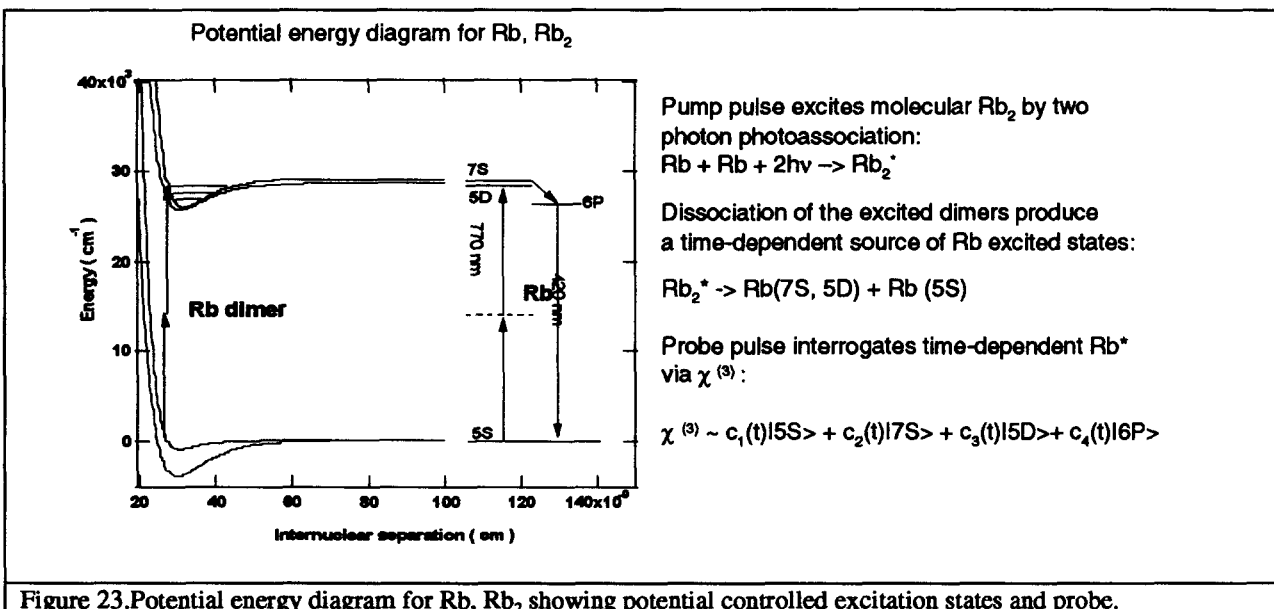


Figure 23. Potential energy diagram for Rb,  $\text{Rb}_2$ , showing potential controlled excitation states and probe.

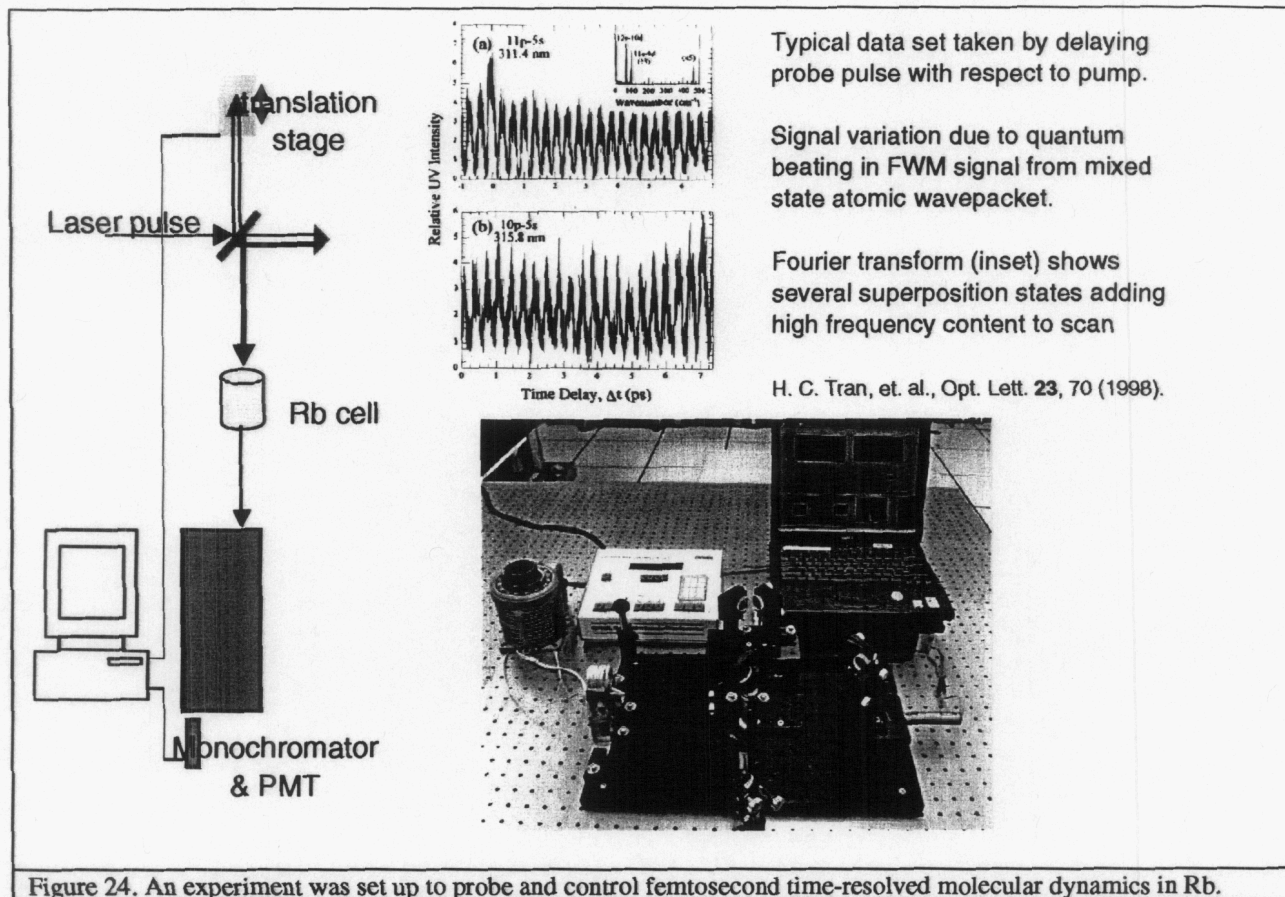


Figure 24. An experiment was set up to probe and control femtosecond time-resolved molecular dynamics in Rb.

#### IV. Summary

We activated the first stage of a planned three-stage optical parametric amplifier (OPA) that would ultimately produce sub-3 fs pulses. Active control with a learning algorithm was implemented to optimize the continuum generated in an argon-filled capillary and to control and optimize the final compressed pulse temporal shape. A collaboration was initiated with Gary Eden's group at U. Illinois to coherently control the population of different states upon dissociation of  $\text{Rb}_2$ . Except for one final optic, a pulse compressor and diagnostics were constructed to produce and characterize pulses in the 5-fs range from the first OPA stage. Unfortunately, the project ended before we could compress this stage and activate the two remaining stages. Although very challenging to implement, this technology would have enabled a wide range of novel applications and basic-science investigations.

## V. References

1. U. Morgner, et al., "Sub-two-cycle pulses from a Kerr-lens mode-locked Ti:sapphire laser", *Opt. Lett.* **24**, 411 (1999).
2. J. K. Ranka, R. S. Windeler, and A. J. Stentz, "Visible continuum generation in air-silica microstructure optical fibers with anomalous dispersion at 800 nm", *Opt. Lett.* **25**, 25 (2000).
3. M. Nisoli, S. De Silvestri, O. Svelto, R. Szipocs, K. Ferencz, Ch. Spielmann, S. Sartania, and F. Krausz, "Compression of high-energy laser pulses below 5 fs", *Opt. Lett.* **22**, 522 (1997).
4. I. Jovanovic, C. A. Ebberts, B. C. Stuart, M. R. Hermann, and E. C. Morse, "Nondegenerate optical parametric chirped pulse amplification", Conference on Lasers and Electro-Optics, Long Beach, California, May 7-11, 2002.
5. A. Poppe, et al., "Few-cycle optical waveform synthesis", *Appl. Phys. B* **72**, 373 (2001).
6. Rick Trebino, Georgia Institute of Technology, private communication (2002).
7. L. Gallman, et al., "Characterization of sub-6-fs optical pulses with spectral interferometry for direct electric-field reconstruction," *Opt. Lett.* **24**, 1314 (1999).
8. P. O'Shea, M. Kimmel, X. Gu, and R. Trebino, "Increased-bandwidth in ultrashort-pulse measurement using an angle-dithered nonlinear-optical crystal", *Opt. Exp.* **7**, 342 (2000).
9. T.C. Weinacht, et al., "Coherent learning control of vibrational motion in room temperature molecular gases", *Chem. Phys. Lett.* **344**, 333 (2001).